

Learning Edge Representations via Low-Rank Asymmetric Projections

Sami Abu-El-Haija
Google Research
Mountain View, California
haija@google.com

Bryan Perozzi
Google Research
New York City, New York
bperozzi@acm.org

Rami Al-Rfou
Google Research
Mountain View, California
rmyeid@google.com

ABSTRACT

We propose a method for learning continuous-space vector representation of graphs, which preserves directed edge information. Previous work in learning structure-preserving graph embeddings learn one embedding vector per node. In addition to learning node embeddings, we also model a directed edge as a learnable function of node embeddings, which enable us to learn more concise representations that better preserve the graph structure. We perform both intrinsic and extrinsic evaluations of our method, presenting results on a variety of graphs from social networks, protein interactions, and e-commerce. Our results show that learning joint representations learned through our method significantly improves state-of-the-art on link prediction tasks, showing error reductions of up to 66% and 16%, respectively, on directed and undirected graphs, while using representations with 8 times less dimensions per node.

1 INTRODUCTION

Recent advancements in learning embeddings of discrete inputs has resulted in a proliferation of methods which learn continuous space representations of graphs. These approaches process a graph and encode each node as a real-valued feature vector, enabling easy integration with existing machine learning algorithms. Structure-preserving embedding methods represent nodes in a continuous vector space, such that two nodes have large similarity (/ small distance) if they are strongly connected in the source training graph. The strength of connection can be binary (e.g. adjacency matrix of an unweighted graph) or continuous. Traditional eigen methods [1, 6, 18] learn embeddings that minimize the euclidean distance of connected nodes, which can be solved (under orthonormal constraints) by eigen-decomposition of the symmetric graph Laplacian. Recent random-walk embedding methods [5, 16] learn representations which encode the random walk transition matrix. These methods embed two nodes close if they co-occur frequently in short random walks. In general, random-walk methods general outperform “eigen” methods on producing vector representations

However, these new random-walk neural methods have two shortcomings. First, these methods do not explicitly model edges. This *node-centric* assumption represents an edge (u, v) identically to reverse counterpart (v, u) , and is unable to capture asymmetric relationships. Second, to preserve the graph structure they embed nodes into a relatively high-dimensional space, sometimes producing an embedding dictionary larger than the sparse adjacency matrix.

In this work we propose to address these limitations by explicitly modeling edges in the network as a function of the nodes. Specifically, we model edges by (i) using a Deep Neural Network (DNN) to map nodes on a low-dimensional manifold, (ii) defining an edge function which represents an edge using the manifold coordinates of its two nodes, and (iii) jointly-optimizing the edge function and the manifold by maximizing the graph likelihood, which we define as a product of the edge function over all node pairs.

More formally, we learn an embedding vector $Y_u \in \mathbb{R}^D$ for every graph node u , a manifold-mapping Deep Neural Network (DNN) $f : \mathbb{R}^D \rightarrow \mathbb{R}^d$ that is shared across all nodes, and an asymmetric edge function $g(u, v) = f(Y_u)^T \times M \times f(Y_v)$ to represent edges in the graph. We learn a low-rank approximation of $M = L \times R$, where both $L \in \mathbb{R}^{d \times b}$ and $R \in \mathbb{R}^{b \times d}$ project the node manifold coordinates to smaller space \mathbb{R}^b . Since b is much smaller than D , we are able to reduce the final node embedding significantly. Figure 1 shows a depiction of our architecture, which is end-to-end differentiable. Our desired likelihood is quadratic but we estimate it with a tractable linear objective using negative sampling, similar to [13].

We find that explicitly modeling edges can drastically reduce the representation dimensionality, for both directed and undirected graphs, especially when coupled with a Deep Neural Network. Further, modeling asymmetry by representing edge (u, v) differently

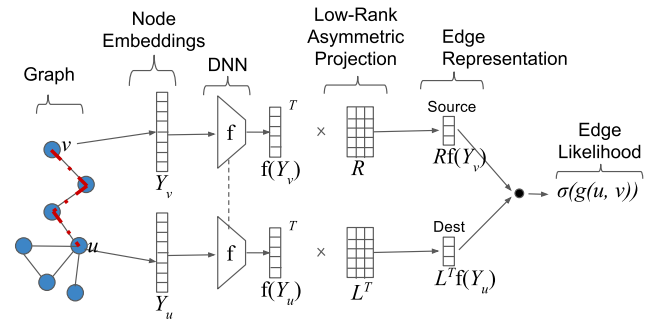


Figure 1: Depiction of our method. On the left: a graph, showing a random walk in dotted-red, where nodes u, v are “close” in the walk (i.e. within the configurable context window). We access the trainable embeddings Y_u and Y_v for the nodes and feed them as input to Deep Neural Network (DNN) f . The DNN outputs manifold coordinates $f(Y_u)$ and $f(Y_v)$ for nodes u and v , respectively. A low-rank asymmetric projection transforms $f(Y_u)$ and $f(Y_v)$ to their source and destination representations, which are used by g to represent an edge.

than (v, u) gives an additional performance boost when preserving the structure of directed graphs. We perform an extrinsic evaluation of our method, by comparing it to the state-of-the-art on link-prediction tasks over a variety of graphs from social networks, biology, and e-commerce. We show that we can consistently learn orders of magnitude smaller embedding dimensions, while improving ROC-AUC metrics. We perform intrinsic evaluations, by training and rendering L2-normed, two-dimensional embeddings of social graphs, which we use to gain intuition on placement choices made by our model.

To summarize, our contributions are as follows. (1) We propose to explicitly model a directed edge function, which we define as low-rank affine projections on a manifold that is (2) produced by a Deep Neural Network (i.e. “deep embeddings”). Together, these two modeling aspects (3) significantly improve the state-of-art on learning continuous graph representations, especially on directed graphs, while producing significantly smaller representation spaces, as evaluated on six graph datasets. For example, we reduce the error on directed graphs by up to $\approx 70\%$ and undirected graphs by up to $\approx 50\%$ when using same-sized representations. However, when our model is restricted to representations which are *8 times smaller* than the baselines, we reduce the error in some cases by up to 66% on directed graphs and 16% on undirected graphs.

2 EDGE REPRESENTATIONS

The typical approach taken by a continuous space graph representation technique associates each node $u \in V$ with its own representation, $Y_u \in \mathbb{R}^D$. Relationships between nodes u and v are captured in a very coarse way, through the use of a distance measure (e.g. $dist(Y_u, Y_v)$). This *node-centric* modeling assumes that all relationships in the graph are symmetric – a limiting assumption which fails to capture any directed relationships.

We seek to better model the complex asymmetry which occurs in many real world graphs. Specifically, given two nodes, u and v , we desire that their distances are allowed to differ ($dist(Y_u, Y_v) \neq dist(Y_v, Y_u)$) to reflect ordering in directed relationships (such as *follower* and *followee* on Twitter). In addition, the asymmetry can also model degree variance in undirected graphs. Consider a popular node m , then the optimization could make $dist(Y_u, Y_m)$ small for all u but not necessarily $dist(Y_m, Y_u)$.

Ideally, we could model this asymmetric behavior by learning representations of all possible pair-wise relationships (u, v) . These representations $Y_{(u,v)}$ could then be used as features for predicting information about an edge such as its presence (i.e. in link prediction). Unfortunately, such direct modeling is prohibitive in practice, as the space of all possible relations grows quadratically with the number of nodes $O(|V|^2)$.

Instead, we propose a much more scalable procedure: to learn a deep function of the nodes which parameterizes the directed link structure of the graph. Specifically, we learn asymmetric transformations of the nodes, which generates for a node u , two representations: one when it is the source of a directed edge, $\hat{Y}_u^{\text{source}}$ and one when it is a destination, \hat{Y}_u^{dest} . At lower levels of the network the representations share parameters, as $\hat{Y}_u^{\text{source}} := L^T \times f(Y_u)$ and $\hat{Y}_u^{\text{dest}} := R \times f(Y_u)$. These representations can be combined for

Algorithm 1 Extract Random Walks

```

Input:  $G = (V, E)$ ,  $n$  (walks per node),  $\tau$  (walk length).
Output: walks.
 $\pi = \text{makeTransitionPr}(E)$ 
walks = []
for  $u \in V$  do
    for  $i = 0$ ;  $i < n$ ;  $i++$  do
        walk = [ $u$ ];
        for  $j = 0$ ;  $j < \tau$ ;  $j++$  do
            curr = walk[-1]
             $v = \text{sampleNext}(curr, \pi)$ 
            walk.append( $v$ )
        end for
        walks.append(walk)
    end for
end for

```

any pair of nodes to model the strength of their directed relationships. That is, for nodes u and v , we represent (u, v) and (v, u) as $dist(\hat{Y}_u^{\text{source}}, \hat{Y}_v^{\text{dest}})$ and $dist(\hat{Y}_v^{\text{source}}, \hat{Y}_u^{\text{dest}})$, respectively.

3 PRELIMINARIES

3.1 Link Prediction

Link prediction is a problem of inferring missing edges in a graph. Link prediction algorithms are trained on a subset of edges E_{train} and are then evaluated on how well they predict the held-out edges E_{test} . Informative graph representations should be able to recover the original graph structure and also infer missing edges. Therefore, we use this task as the benchmark for evaluating the quality of our learned representations.

3.2 Graph Embedding

Graph embedding approaches learn a D -dimensional embedding dictionary $Y \in \mathbb{R}^{|V| \times D}$, containing continuous real-valued vector $Y_u \in \mathbb{R}^D$ for every graph node $u \in V$. Earlier approaches in computing embeddings include Eigenmaps [1] with the objective:

$$\min_Y \sum_{(u,v) \in E} A_{uv} \|Y_u - Y_v\|_2^2 \quad \text{s.t.} \quad Y^T \mathbf{D} Y = I, \quad (1)$$

where the weight of edge (u, v) is stored in the adjacency matrix at A_{uv} and \mathbf{D} is a diagonal weight matrix with $D_{vv} = \sum_u A_{uv}$. This optimization yields an embedding space where Y_u and Y_v are near if A_{vu} is large (or non-zero). Equation (1) also appears in equivalent forms in [6, 18]. Furthermore, Bregman Iterations has been proposed to optimize an L1-formulation of the above objective function [22].

3.3 DeepWalk and node2vec

Rather than operating directly on the adjacency matrix A , DeepWalk [16] and node2vec [5] extend a node’s direct neighbors to include nodes that are within small number of hops. They sample many random walks from the graph. If nodes u and v are appear frequently close in the random walks (within a few hops, less than context window size), then inner product of $\langle Y_u, Y_v \rangle$ would be a large positive value. Algorithm 1 extracts random walks. It begins by computing

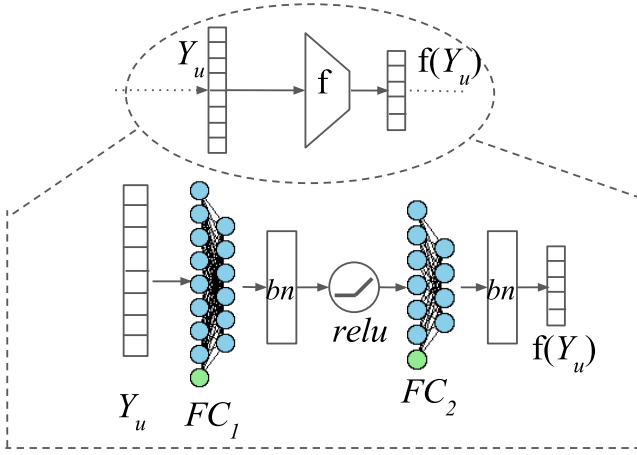


Figure 2: Depiction of f_θ , where $\text{FC}_i(x) = \mathbf{W}_i x + b_i$ is a fully-connected layer with weight matrix \mathbf{W}_i and bias vector b_i , bn is BatchNorm [8] and $\text{relu}(x) = \max(0, x)$ is an element-wise activation function.

a probability transition matrix π , where π_{uv} indicates the probability of walker visiting node v conditioned on current node being u . Node2vec [5] uses a second-order probability transition function containing π_{tuv} , where the probability of walker visiting node v is conditioned on current node u and previous node t . Node2vec’s random walk use hyper-parameters p and q , which effectively yield a graph traversal algorithm that’s like an interpolation between Depth-First Search (DFS) and Breadth-First Search (BFS). We refer the reader to [5] for further details. We adopt this method for generating random walks in our work.

After sampling random walks, DeepWalk and node2vec treat each walk ($u_1 \rightarrow u_2 \rightarrow \dots \rightarrow u_\tau$) as a sentence “ $u_1 u_2 \dots$ ” where node IDs become textual words. Then they use the word2vec algorithm [13] to compute embeddings per word (i.e. node). They show that these learned embeddings are useful for link prediction and node classification tasks. Our learning framework differs from word2vec in two important ways; First, we optimize the graph likelihood and train jointly node embeddings and the edge function (See Section 4); Second, we define the “context” for directly graph differently than undirected ones. Specifically, a random walk $u_1 \rightarrow u_2 \rightarrow u_3 \rightarrow u_4 \rightarrow u_5$ would produce $\{u_1, \dots, u_5\}$ as a context of u_3 if graph is undirected and $\{u_4, u_5\}$ if the graph is directed.

4 OUR METHOD

4.1 Model

Given an (un)directed graph $G = (V, E)$, we learn an embedding vector $Y_u \in \mathbb{R}^D$ for each node $u \in V$. We learn a Deep Neural Network (DNN) $f_\theta : \mathbb{R}^D \rightarrow \mathbb{R}^d$ that maps a node onto a low-dimensional manifold. f_θ is depicted in Figure 2, and is defined as:

$$\begin{aligned} f_\theta : Y_u &\rightarrow \text{FC}_{\{\mathbf{W}_1, b_1\}} \rightarrow \text{BatchNorm} \rightarrow \text{relu} \\ &\rightarrow \text{FC}_{\{\mathbf{W}_2, b_2\}} \rightarrow \text{BatchNorm} \rightarrow f_\theta(Y_u), \end{aligned}$$

where $\text{FC}_{\{\mathbf{W}, b\}}$ is a fully-connected layer with weight matrix \mathbf{W} and bias vector b , BatchNorm is described in [8], $\text{relu}(x) = \max(0, x)$ is an element-wise activation function, and $\theta = \{\mathbf{W}_1, b_1, \mathbf{W}_2, b_2, \dots\}$.

In addition, we define a general class of edge functions $g(u, v) \in \mathbb{R}$ where symmetricity is not imposed, yielding $g(u, v) \neq g(v, u)$. Consider a low-rank affine projection in the manifold space:

$$g(u, v) = f(Y_u)^T \times M \times f(Y_v), \quad (2)$$

where low-rank projection matrix $M = L \times R$ with $L \in \mathbb{R}^{d \times b}$ and $R \in \mathbb{R}^{b \times d}$. We refer to b as the bottleneck dimension and we experiment with $b < d < D$. We can factor $g(u, v)$ into an inner product $\langle L^T f(Y_u), R f(Y_v) \rangle$. We refer to $L^T f(Y_u) \in \mathbb{R}^b$ and $R f(Y_v) \in \mathbb{R}^b$, respectively, as the left- and right-asymmetric embeddings.

It is natural to question: Why do we need $f()$? Since we are learning Y jointly with f , why not skip f and directly learn its output? Indeed, $f()$ removes degrees of freedom from the embedding (e.g. relu activation and BatchNorm) the training objective function can be better minimized if we skip f .

A natural extension of the equation (2) is to use a combination of multiple low-rank affine projections, as:

$$g^{(2)}(u, v) = \langle w_g^{(2)}, [\text{relu}(g_1(u, v)), \dots, \text{relu}(g_h(u, v))] \rangle, \quad (3)$$

where $w_g^{(2)} \in \mathbb{R}^h$ a parameter vector of the output layer, h is the number of projections, and each projection g_i has its own $L_i \in \mathbb{R}^{d \times b}$ and $R_i \in \mathbb{R}^{b \times d}$. Even though there total size of parameters for Y, f, g may be large, we can have a low memory footprint during inference if we precompute $L^T f(Y_u)$ and $R f(Y_u)$ for every $u \in V$.

4.2 Graph Likelihood

Given a training graph $G = (V, E_{\text{train}})$, one can define a probability measure as a product of an edge estimate Q on all node pairs:

$$\Pr(G) = \prod_{(u, v) \in E_{\text{train}}} Q((u, v)) \prod_{(u, v) \notin E_{\text{train}}} 1 - Q((u, v)), \quad (4)$$

where Q is a trainable edge estimator. If Q is a perfect estimator, then it should output 1 on all $(u, v) \in E$ and should output 0 on all $(u, v) \notin E$, which makes $\Pr(x) = 1$ iff $x = G$. An equivalent form of equation 4 is:

$$\prod_{\substack{u \in V \\ v \in V}} Q((u, v))^{\mathbb{1}[(u, v) \in E_{\text{train}}]} (1 - Q((u, v)))^{\mathbb{1}[(u, v) \notin E_{\text{train}}]} \quad (5)$$

where indicator function $\mathbb{1}[x] = 1$ if predicate x is true and = 0 otherwise. Note that two product terms are exclusive.

Recent work show that extending the neighbor-set of nodes beyond their direct connections via random walks, can improve generalization of prediction tasks such as link-prediction and node classification [5, 15, 16]. Following this motivation, we propose to replace the binary edge presence $\mathbb{1}[(u, v) \in E_{\text{train}}]$ in equation (5) by simulated random walk statistics, and formulate our full quadratic graph likelihood as:

$$\Pr(G) \propto \prod_{\substack{u \in V \\ v \in V}} \sigma(g(u, v))^{\mathcal{D}_{uv}} (1 - \sigma(g(u, v)))^{\mathbb{1}[(u, v) \notin E_{\text{train}}]} \quad (6)$$

where $\sigma(x) = 1/(1 + \exp(-x))$ is the standard logistic, the edge function g is described in section 4.1, and \mathcal{D}_{uv} is the unnormalized

frequency that nodes u and v appear within the configured context window, in simulated random walks [16]. Note that our likelihood in equation (6) is not standard, especially that the two terms are not exclusive, as it is possible for both conditions $\mathcal{D}_{uv} > 0$ and $(u, v) \notin E_{\text{train}}$ to be simultaneously true. It follows that the expression under the product-operator is in $[0, 1]$ since the logistic $\sigma : \mathbb{R} \rightarrow [0, 1]$. We use *proportional to* \propto instead of equality since the normalizing constant $\int_G \Pr(G)$ is only a scaling factor and should not change the arg max of the likelihood. Our experiments show that the likelihood yields a powerful representation for preserving the graph structure, as evaluated on link-prediction tasks.

Although a naive optimization of equation (6) is quadratic, \mathcal{D} is sparse with $O(|V|)$ non-zero entries, making it possible to compute the first term in equation (6) in linear time. Further, we use Noise Contrastive Estimation (NCE, section 4.4) to estimate the product over $(u, v) \notin E$, which is important in many real applications where graphs are large and most edges are negative, having $|\{(u, v) : u, v \in V \text{ and } (u, v) \notin E\}| \approx O(|V|)$.

4.3 Training Data Generation

4.3.1 Positives. Given a graph $G = (V, E)$, we take a partition $E_{\text{train}} \subset E$ and extract random walks from E_{train} using Algorithm 1. Starting from every node u_1 , we simulate n random walks, each of length τ , like:

$$u_1 \rightarrow u_2 \rightarrow u_3 \rightarrow \dots \rightarrow u_\tau.$$

Then, for every walk, we extract all node pairs within the context window, similar to [13].

$$(u_i, u_j) \quad \forall j \in \mathbb{Z}, i - w_l \leq j \leq i + w_r, j \neq i, \quad (7)$$

where w_l and w_r are the context window left and right offsets. For example, for an undirected graph, if we use context window of size 5, then $w_l = w_r = 2$ and therefore $j \in \{-2, -1, 1, 2\}$. Extracting positive pairs yields a list \mathcal{D} that contain duplicates and over-load notation by defining \mathcal{D}_{uv} as the frequency of (u, v) in list \mathcal{D} . It is trivial to show that the number of pairs is linear in $|V|$:

$$|\mathcal{D}| = n\tau O((w_l + w_r)(\tau - (w_l + w_r + 1))|V|) = O(|V|) \quad (8)$$

4.3.2 Negatives. We fix a set of negatives for every node. Before training, for every node u , we create its negative set \bar{u} as:

$$\bar{u} = \{v_1^-, v_2^-, \dots\} \quad \text{s.t.} \quad \forall v^- \in \bar{u}, (u, v^-) \notin E_{\text{train}} \quad (9)$$

where elements of \bar{u} are sampled uniformly at random. Arguably, it is possible to increase the accuracy of our models if we sub-sample frequent nodes (i.e. with a high degree) as recommended by [13], however, we leave this as future work. In our training loop, we uniformly sample a subset of size K from \bar{u} , where K is a hyper-parameter for Noise Contrastive Estimation (NCE). We use a fixed $K = 5$ for all our experiments.

4.4 Negative Sampling

We define a linear objective \mathcal{L} using negative sampling, similar to (section 2.2 of [13]), as an approximation to the quadratic graph

likelihood (6), as:

$$\mathcal{L} = \mathbb{E}_{(u, v) \sim \mathcal{D}/Z} \left[\log \sigma(g(u, v)) + \sum_{v^- \in \text{Sample}(K, \bar{u})} \log(1 - \sigma(g(u, v^-))) \right], \quad (10)$$

where $\text{Sample}(K, \bar{u})$ uniformly samples K negatives from \bar{u} without replacement and Z is a normalizing constant. Note that the outer expectation $(u, v) \in \mathcal{D}$ is linear and the inner summation goes over K items. We use TensorFlow [19] to obtain the gradients $\frac{\partial \mathcal{L}}{\partial Y_u}, \frac{\partial \mathcal{L}}{\partial \theta}, \frac{\partial \mathcal{L}}{\partial L}, \frac{\partial \mathcal{L}}{\partial R}$ for each mini-batch. We use ADAM [10] with a fixed learning-rate to optimize θ, f, g , and use Stochastic Gradient Descent (SGD) to optimize embeddings Y . We only update the anchor embeddings Y_u during the gradient steps on the objective \mathcal{L} , as preliminary experiments showed that we get better performance this way.

5 EXPERIMENTS

5.1 Link Prediction

We follow the setup in [5] for link prediction. First given a graph $G = (V, E)$ we partition its edges into two equal size disjoint partitions E_{train} and E_{test} , such that, E_{train} is connected. Second, we sample negative edges for training and testing, E_{train}^- and E_{test}^- , where E_{train}^- is sampled from the compliment of E_{train} and E_{test}^- is sampled from the compliment of E . All four train/test edge sets are of equal size. Third, we simulate random walks on E_{train} to get \mathcal{D} , using algorithm 1 and equation 7. Fourth, only for directed graphs, we extend E_{test}^- to contain all edges (v, u) s.t. $(u, v) \in E$ and $(v, u) \notin E$. Finally, we train each algorithm and we evaluate ROC-AUC metrics on their ranking of $(E_{\text{test}}, E_{\text{test}}^-)$.

5.1.1 Datasets. We test our algorithms on 4 undirected datasets and 2 directed datasets. We obtain PPI from [5] and the other five datasets from Stanford SNAP [11]. We only use the largest weakly connected component (WCC) from the original graph. The statistics and dataset description are as follows:

Directed graphs:

- (1) **soc-opinions:** A social network $|V| = 75,877$ and $|E| = 508,836$. Each directed edge represents whether a user trusts the opinion of another.
- (2) **wiki-vote:** A voting network with $|V| = 7,066$ and $|E| = 103,663$. Nodes are Wikipedia editors. Each directed edges represents a vote that another becomes an administrator.

Undirected graphs:

- (1) **ca-HepTh:** A citation network of High Energy Physics Theory from Arxiv, with $|V| = 17,903$ and $|E| = 197,031$. Each undirected edge represents co-authorship between two author nodes.
- (2) **ca-AstroPh:** A citation network of Astrophysics from Arxiv, with $|V| = 17,903$ and $|E| = 197,031$. Each undirected edge represents co-authorship between two author nodes.
- (3) **ego-Facebook:** A small portion of the Facebook social network, with $|V| = 4,039$ and $|E| = 88,234$. The nodes are users and the edges indicate friendship. We note that this graph is

Dataset	Adjacency Methods			Embedding Methods									
	Non-Embedding baselines			d	Embedding Baselines			Ours: (end-to-end) Graph Likelihood					
directed	Jaccard	Common Neighbors	Adamic Adar		Eigen Maps	node2vec	DNGR	Symmetric shallow	Symmetric deep	Asymmetric shallow	Asymmetric deep	% Error Reduction	
	soc-epinions	0.649	0.649	0.647	8	†	0.617	†	0.694	0.665	0.695	0.825	54.4%
					16	†	0.672	†	0.710	0.713	0.699	0.840	51.1%
					32	†	0.665	†	0.740	0.713	0.700	0.845	53.8%
					64	†	0.668	†	0.766	0.722	0.698	0.834	50.1%
	wiki-vote	0.579	0.580	0.562	8	0.613	0.557	0.630	0.603	0.602	0.608	0.871	65.0%
					16	0.607	0.582	0.622	0.623	0.639	0.643	0.900	73.4%
					32	0.600	0.579	0.619	0.642	0.661	0.683	0.911	76.6%
					64	0.613	0.575	0.598	0.660	0.672	0.702	0.917	78.5%
undirected	ca-HepTh	0.765	0.765	0.765	8	0.786	0.734	0.706	0.855	0.848	0.605	0.879	43.2%
					16	0.790	0.796	0.780	0.894	0.826	0.885	0.899	50.4%
					32	0.795	0.866	0.829	0.896	0.886	0.884	0.911	33.9%
					64	0.802	0.881	0.868	0.878	0.884	0.870	0.910	24.7%
	ca-AstroPh	0.942	0.942	0.944	8	0.825	0.686	0.852	0.923	0.925	0.592	0.917	44.1%
					16	0.825	0.808	0.877	0.950	0.923	0.657	0.945	55.8%
					32	0.825	0.908	0.917	0.955	0.938	0.942	0.955	46.1%
					64	0.824	0.938	0.939	0.948	0.936	0.936	0.958	30.7%
(4) PPI	ego-Facebook	0.971	0.974	0.976	8	0.977	0.880	0.927	0.969	0.854	0.690	0.971	n/a
					16	0.974	0.923	0.925	0.972	0.943	0.966	0.974	n/a
					32	0.973	0.957	0.970	0.972	0.959	0.963	0.976	10.9%
					64	0.964	0.968	0.981	0.969	0.961	0.961	0.976	n/a
					8	0.710	0.640	0.583	0.746	0.763	0.550	0.804	32.4%
					16	0.711	0.620	0.687	0.780	0.772	0.786	0.817	36.7%
					32	0.709	0.639	0.741	0.779	0.784	0.794	0.833	35.5%
					64	0.707	0.664	0.767	0.791	0.767	0.813	0.837	30.0%

Table 1: Link Prediction results from ranking E_{test} across six graph datasets. Numbers shown are the ROC-AUC. Row-wise: the first two datasets are directed and the last four are undirected graphs. Column-wise: The first three methods are adjacency (non-embedding) methods that use the direct neighbors of u and v for computing $g(u, v)$. We then list all embedding methods, preceded by d , the dimensionality of the learned embeddings. We report three embedding methods followed by our four embedding methods. We compare embedding methods across different dimensionality $\{8, 16, 32, 64\}$, marking in bold the top performer for the given dimensionality. For asymmetric embedding methods, we train with half of the dimensionality ($\{4, 8, 16, 32\}$) since in practice we need to store both sides of the embedding to compute an edge score, therefore every row contains the same total dimensions per node. The last column shows the relative reduction in error of our Asymmetric Deep model compared the best baseline, and we report “n/a” when there is no error reduction (i.e. baseline outperforms our asymmetric deep embedding method). Symbol † indicates that the algorithm runs out of memory, as the dense transformations of adjacency matrix are larger than our machine’s memory (32 GB).

an ego-network graph, which contains only the complete social connections of 10 seed users. We analyze this unique structure further through visualization in Section 5.2.

(4) **PPI:** A protein-protein interaction graph, with $|V| = 3,852$ and $|E| = 20,881$. This is a challenging real-world dataset, where each node is a protein and an edge represents that two proteins interact.

5.1.2 Methods. We report results from various methods, including baselines that use the entire train graph for inference, baselines that learn embeddings and use them for inference, and our proposed models.

Adjacency (non-embedding) Baselines:

These methods require E_{train} during inference. Let $N(u)$ denote the list of direct neighbors to node u , that are observed according to

E_{train} . If the graph is directed, then $N(u)$ only stores outgoing edges. Equivalently, $N(u)$ can be set to the non-zero entries for row u in the graph’s adjacency matrix. We include performance metrics from baselines the score of edge (u, v) as a function of $N(u)$ and $N(v)$. In particular, we run the following baselines:

(1) **Jaccard Coefficient** models the edge score as

$$g(u, v) = \frac{|N(u) \cap N(v)|}{|N(u) \cup N(v)|}$$

(2) **Common Neighbors** models the edge score as

$$g(u, v) = |N(u) \cap N(v)|$$

(3) **Adamic Adar** models the edge score as

$$g(u, v) = \sum_{x \in N(u) \cap N(v)} \frac{1}{\log(|N(x)|)}$$

Embedding Baselines:

These methods use E_{train} to learn embedding Y_u for every graph node u . During inference, they use the learned embedding dictionary Y but *not* the original graph edges. We compare against various state-of-the-art embedding methods.

- (1) **Laplacian EigenMaps** which finds the lowest eigenvectors of the graph Laplacian matrix [1] The eigendecomposition is real iff the Laplacian is symmetric. Therefore, we convert directed graphs to undirected ones during training. During inference, we define the edge scoring function as $g(u, v) = -||Y_u - Y_v||$.
- (2) **node2vec** learns embedding by simulating random walks on E_{train} and minimizing a hierarchical softmax objective [5]. We use the author’s code to learn node embeddings, then we calculate the hadamard product $Y_u \odot Y_v$ for all node pairs (u, v) in E_{train} or E_{train}^- . Finally, we model an edge score as $g(u, v) = w(Y_u \odot Y_v)$ where w is trained using off-the-shelf binary classification algorithm, scikit-learn’s Logistic Regression. We train w so that the $\sigma(w(Y_u \odot Y_v)) \approx 0$ if $(u, v) \in E_{\text{train}}$ and ≈ 1 if $(u, v) \in E_{\text{train}}^-$. According to our understanding, this is similar to how node2vec performed link prediction [5].
- (3) **DNGR** learns a non-linear (i.e. deep) node embeddings by passing “smoothed” adjacency matrix through a deep auto-encoder [?]. The “smoothing” (called Random Surfing in [?]) is their proposed alternative to random walks, which effectively has a different context weighing from node2vec. We use the author’s code to train the auto-encoder on the adjacency matrix that corresponds to E_{train} . To test different embedding sizes, we only change the size of the last bottleneck layer in their code and keep the remainder of default architecture. We then output the bottleneck layer values for all nodes to a file and use them for the link prediction task, with scoring function $g(u, v) = Y_u^T Y_v$.

Our Methods:

- (1) **Symmetric Shallow:** $w^T()$. This model is similar to node2vec, except that the model parameters Y and w are jointly trained on our objective 10.
- (2) **Symmetric Deep:** $w^T(f(Y_u) \odot f(Y_v))$. Similar to above, except that the embedding representation is deep.
- (3) **Asymmetric Shallow:** $Y_u^T \times L \times R \times Y_v$. Applying asymmetry directly on the embeddings without a DNN.
- (4) **Asymmetric Deep:** $f(Y_u)^T \times L \times R \times f(Y_v)$. Our full asymmetric formulation, when composed of a single affine projection. For both of our asymmetric methods, after training Y, f_θ, g , we use only the b -dimensional edge representations for inference ($L^T Y_u$ and $R Y_u$).

We train all our models on \mathcal{D} using learning rates [0.001, 0.01, 0.1] with L2 regularization of 0.0001 on all trainable parameters. We do model selection using E_{train} and E_{train}^- .

5.1.3 Link Prediction Results. Here we discuss the results of our link prediction experiment, which are presented in Table 1.

First we turn our attention to the directed graphs, where there is a dramatic increase in performance. Specifically on graph soc-epinions, the asymmetric deep model reduces error over the baseline by 50.4% for 128-dimensional representations. We see that the asymmetric deep representations make more efficient use of their

allocated space than the baseline, and therefore have even larger relative reduction in error when d is lowered (up to 54.4% improvement, when $d = 8$). The second directed graph, wiki-vote, shows an even stronger performance increase, with a reduction in error of up to 80.3% (a 59.3% improvement in AUC over the state-of-the-art baseline).

Next, we consider the undirected graphs. On the citation networks, ca-HepTh and ca-AstroPh, we see that deep asymmetric approaches offer large improvements over the baseline when $d = 8$ (respectively, 73.8% and 75.5%), but this lead narrows as the baseline representations are allowed more capacity. On the Facebook graph, we observe a similar pattern of behavior. As noted earlier, the Facebook graph has a very distinctive structure, which makes it easy to predict links on – most of the edges in the graph involve connections to the 10 ‘seed’ users who created the dataset. On this graph, the node2vec baseline fails to outperform the hand-engineered link prediction features. However, our deep asymmetric approach is still competitive. Finally, we examine results on the protein-protein interaction network. This is perhaps our most challenging undirected graph, derived from a problem of significant scientific interest. On this network, we observe a large boost from the deep asymmetric model over the baseline method, of up to a 51.5% relative reduction in error ($d = 64$). We note that even when using representations which are 16 times smaller ($d = 8$), the deep asymmetric model has AUC of 0.8039, which is a 36.3% reduction in error over the best node2vec baseline ($d = 128$, with AUC of 0.6918).

We comment briefly on other observations from methods which optimize the graph likelihood. First, from a modeling prospective, our shallow symmetric formulation is identical to node2vec’s, but they differ in the training objective. This verifies that our proposed graph likelihood produces embeddings that better preserve the graph structure than the hierarchical softmax objective. Second, shallow models tend to perform much worse in the presence of limited representation size. This is unsurprising, as the limited representation size directly effects the capacity of a smaller model. Third, using asymmetry alone (without a deep model) does not offer nearly as much performance improvement as the asymmetric deep model.

5.2 Manifold Visualizations

We visualize embeddings learned for link prediction for the facebook network. Although we only used E_{train} to train the embedding, we show both E_{train} and E_{test} on the visualization. Figure 3 shows embeddings. We trained those 2-dimensional embeddings by choosing $b = 2$ and setting L2-norm constraints on both sides of the asymmetric embeddings, specifically: $||L^T f(Y_u)||_2 = ||R f(Y_v)||_2 = 1$. Under this constraint, those 2-dimensional embeddings have only one degree of freedom e.g. angle, and it is straight-forward to show that

$$\arg \max_v \langle L^T f(Y_u), R f(Y_v) \rangle = \arg \min_v ||L^T f(Y_u) - R f(Y_v)||$$

5.3 Parameter Sensitivity

In order to understand the impact of the representation size as a function of task performance, we varied the number of dimensions in the model from $d = 4$ to $d = 512$. The results of this experiment are shown in Figure 4.

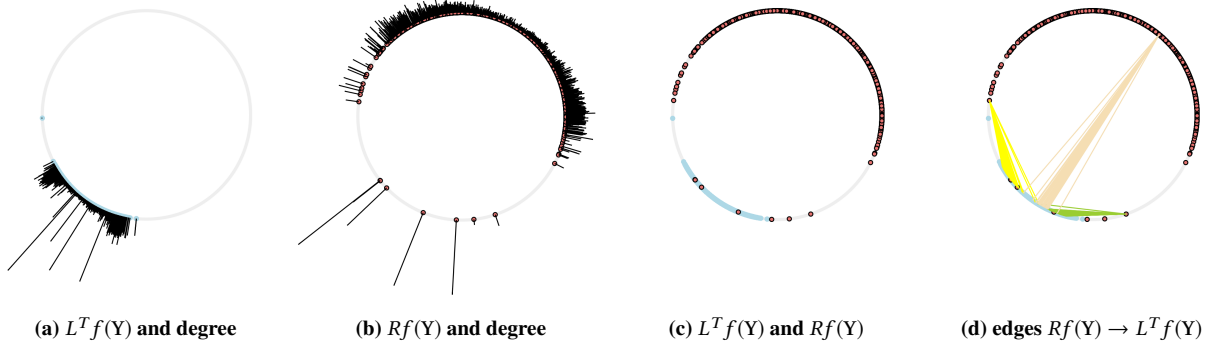


Figure 3: Visualization of 2-dimensional embeddings learned from our Asymmetric Deep model on the Facebook dataset. Columns (a-d) render nodes in their original learned coordinates (mapped to pixel space as $(L^T \times f(Y_u)) * \text{radius} + \text{center}$). Columns (a) and (b), respectively render the left- and right-embeddings of all nodes. Each node is plotted as a circle, with an overlay tick whose length is proportional to its degree. Column (c) combine the left- and right-embedding spaces, dropping the degree ticks for clarity. Plot (d) shows a few selected nodes from the right-embedding, and for each selected node, we draw all its edges to nodes onto the left-embedding. The visualization shows that the asymmetric embedding spaces are almost disjoint, and the high-degree nodes are placed in the right embedding space close to the left embedding manifold, and highest degree nodes are within the left manifold. It seems like those high degree nodes have “pulled” the asymmetric manifold. Overall, nodes are embedded in the right-space close to their neighbors in the left-space. Note that the test AUC of this 2-dimensional norm-constrained model is 80% and can only give us an idea (in paper-print dimensions) about the optimization, as it is inferior to our (slightly higher dimension model scoring > 97% AUC).

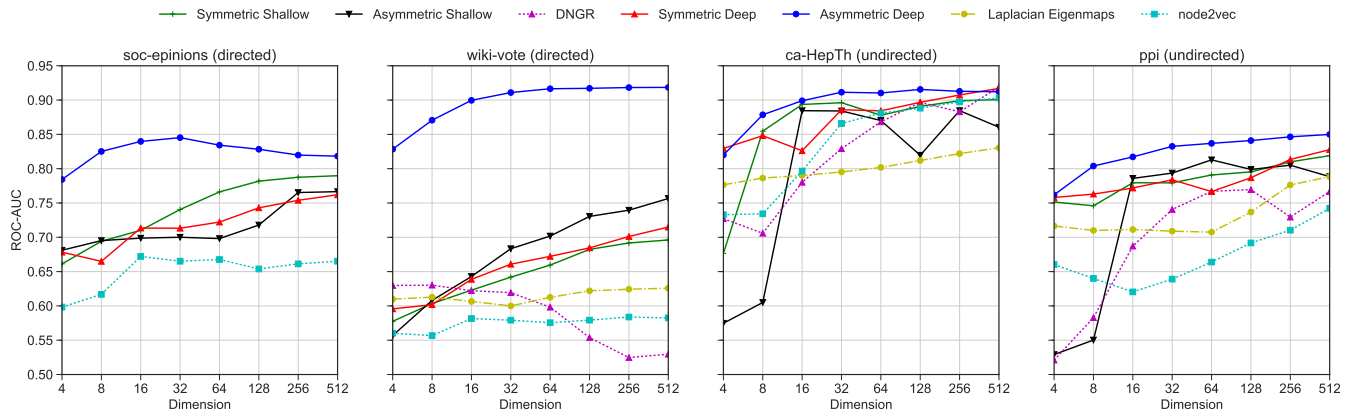


Figure 4: ROC-AUC results for our models versus the baselines measured on a suite of datasets.

6 RELATED WORK

There is a rapidly growing body of literature on applying neural networks to problems which have as input a graph. We divide the related work into several broad groups, based on whether it concerns graph classification (assigning a label to G) or learn a representation per node. Different approaches also consider different transformation of the graph.

Graph-Level Learning: Graph-level learning algorithms aim to predict a label to assign to the entire graph. Duvenaud et al. [4] predict attributes for chemical compounds using its graph representation. They recursively represent each node as a combination of its neighbors. Niepert et al. [14] apply 1-dimensional strided convolution on graphs by mapping graph nodes into an ordered list using a deterministic ordering function (e.g. node degree or centrality). A number of additional methods learn convolutions in the Fourier domain, by

learning filters axis-aligned with the eigenvectors of the graph Laplacian [2, 3, 7]. They assign a graph label given a real-valued input $x \in \mathbb{R}^{|V|}$, one entry per node.

We differ from all graph-level methods, since our goal is to learn a manifold that can reconstruct the graph and infer missing edges rather than assigning one label on the entire graph.

Node-centric Learning: These methods learn a representation per node in the input graph, and are most related to our work here. In fact, our work builds on the approach introduced in [16], which learns node embeddings using simulated random walks. These node embeddings have been used as features in tasks on networks, such as node classification [16], user profiling [17], and link prediction [5]. Some extensions of Deepwalk include node2vec [5], parameterizing the random walk process to allow more focused discovery of structural relationships; author2vec [9], augmenting nodes with bag-of-word

representations for documents; and Tri-Party DNN, modeling heterogeneous graphs with three different node types. Other node-centric methods are concerned with shorter dependencies in the graph Wang et al. [20, 21].

Our work differs from existing random walk methods in three ways. First, we explicitly model asymmetric relationships between nodes. Even though random walk methods we surveyed **respect** edge direction during the walk, they do **not** model edge direction and represent (u, v) identically to (v, u) [5, 9, 12, 16]. This flexibility better models the heterogeneity which occurs in real world networks, where social relationships may not be reciprocal (i.e. the graph is *directed*), or typically have a very unbalanced degree distribution. Second, our node embeddings are produced by a deep neural network (DNN), unlike the shallow (effectively 1-layer) networks previously used. Third, rather than a 2-stage optimization of first training embeddings on random walk sequences, followed by learning a task-specific classifier, we propose a graph likelihood and use it to jointly train the embeddings, the manifold-mapping DNN, and the edge function. Even though the graph likelihood does *not* match a link-prediction loss, it produces superior results on link-prediction using very few dimensions.

7 CONCLUSION

We introduced a method for integrating directed edge information for learning continuous representation for graphs. Our method explicitly models edges as functions of node representations. We jointly optimize the edge function and node representations over a noise-contrastive estimate of the graph likelihood. Our empirical evaluation focused on link prediction tasks using a number of graphs collected from real world applications. Our experimental results show that modeling edges as asymmetric affine projections through the node representation space, helps produce more accurate and compact embedding spaces. In particular, we show that asymmetric edge modeling improves performance over state-of-the-art approaches, especially on directed graphs, reducing error by up to $\approx 70\%$ and $\approx 50\%$, respectively, on directed and undirected graphs while using the same number of dimensions per node. In addition to AUC metric improvements, explicit edge modeling allows us to learn smaller embeddings. The representations learned through our model is more efficient at utilizing the available space. Our embeddings are able to outperform the baseline even when outputting 10x less dimensions per node. We believe that explicitly modeling edge representations addresses a substantial problem in related work, and could enable avenues of future investigation for learning continuous representation of graphs.

REFERENCES

- [1] M. Belkin and P. Niyogi. 2001. Laplacian eigenmaps and spectral techniques for embedding and clustering. In *Advances in Neural Information Processing Systems (NIPS)*.
- [2] Joan Bruna, Wojciech Zaremba, Arthur Szlam, and Yann LeCun. 2013. Spectral networks and deep locally connected networks on graphs. In *International Conference on Learning Representations*.
- [3] Michaël Defferrard, Xavier Bresson, and Pierre Vandergheynst. 2016. Convolutional Neural Networks on Graphs with Fast Localized Spectral Filtering. In *Advances in Neural Information Processing Systems (NIPS)*.
- [4] D. Duvenaud, D. Maclaurin, J. Iparragirre, R. Bombarell, T. Hirzel, A. Aspuru-Guzik, and R. Adams. 2015. Convolutional Networks on Graphs for Learning Molecular Fingerprints. In *Advances in Neural Information Processing Systems (NIPS)*.
- [5] A. Grover and J. Leskovec. 2016. node2vec: Scalable Feature Learning for Networks. In *Proceedings of the 22nd ACM SIGKDD International Conference on Knowledge Discovery and Data Mining*.
- [6] L. Hagen and A. Kahng. 1992. New spectral methods for ratio cut partitioning and clustering. In *IEEE Trans. Computer-Aided Design*.
- [7] Mikael Henaff, Joan Bruna, and Yann LeCun. 2015. Deep Convolutional Networks on Graph-Structured Data. In *arXiv:1506.05163*.
- [8] Sergey Ioffe and Christian Szegedy. 2015. Batch Normalization: Accelerating Deep Network Training by Reducing Internal Covariate Shift. *Journal of Machine Learning Research (JMLR)*.
- [9] G. J. S. Ganguly, M. Gupta, V. Varma, and V. Pudi. 2016. Author2Vec: Learning Author Representations by Combining Content and Link Information. In *Proceedings of the 25th International Conference Companion on World Wide Web (WWW '16 Companion)*.
- [10] Diederik P. Kingma and Jimmy Ba. 2015. Adam: A Method for Stochastic Optimization. *International Conference on Learning Representations (ICLR)*.
- [11] J. Leskovec and A. Krevl. 2014. SNAP Datasets: Stanford large network dataset collection. <http://snap.stanford.edu/data>
- [12] Y. Luo, Q. Wang, B. Wang, and L. Guo. 2015. Context-Dependent Knowledge Graph Embedding. In *Conference on Empirical Methods in Natural Language Processing (EMNLP)*.
- [13] T. Mikolov, I. Sutskever, K. Chen, G. Corrado, and J. Dean. 2013. Distributed representations of words and phrases and their compositionality. In *Advances in Neural Information Processing Systems*.
- [14] M. Niepert, M. Ahmed, and K. Kutzkov. 2016. Learning Convolutional Neural Networks for Graphs. In *International Conference on Machine Learning (ICML)*.
- [15] S. Pan, J. Wu, X. Zhu, C. Zhang, and Y. Wang. 2016. Tri-Party Deep Network Representation. In *International Joint Conference on Artificial Intelligence*.
- [16] B. Perozzi, R. Al-Rfou, and S. Skiena. 2014. DeepWalk: Online Learning of Social Representations. In *Knowledge Discovery and Data Mining*.
- [17] Bryan Perozzi and Steven Skiena. 2015. Exact Age Prediction in Social Networks. (2015), 2 pages.
- [18] J. Shi and J. Malik. 2000. Normalized cuts and image segmentation. In *IEEE Trans. Pattern Anal. Mach. Intell.*
- [19] TensorflowTeam. 2015. TensorFlow: Large-Scale Machine Learning on Heterogeneous Systems. <http://tensorflow.org/> Software available from tensorflow.org.
- [20] D. Wang, P. Cui, and W. Zhu. 2016. Structural Deep Network Embedding. In *Proceedings of the 22nd ACM SIGKDD International Conference on Knowledge Discovery and Data Mining*.
- [21] H. Wang, X. Shi, and D-Y. Yeung. 2017. Relational deep learning: A deep latent variable model for link prediction. In *Conference on Artificial Intelligence (AAAI)*.
- [22] Y. Yu, C. Fang, and Z. Liao. 2015. Piecewise Flat Embedding for Image Segmentation. In *IEEE International Conference on Computer Vision (ICCV)*.